# EXPERIMENTALLY DETERMINING THE INTERNAL FRICTION OF CONDUCTIVE FIBERS

NSF Summer Undergraduate Fellowship in Sensor Technology
Mary Kutteruf (Physics) – Bryn Mawr College
Advisor: Dr. J. J. Santiago-Avilés

## ABSTRACT

Conductive polymer fibers have the potential to take electronics to the molecular scale by allowing current to pass along a single molecule. Unfortunately, their use has been limited by difficulty in determining their mechanical properties. It is the goal of this research to develop a technique for measuring the internal friction of conductive polymer fibers. Unfortunately, I was not able to use a conducting polymer for this research, but instead used gold wire. I forced the wire into harmonic resonance by exposing it to an oscillating magnetic field while passing current along the wire. Using a phototransistor and LED I was able to observe the decay of the fiber from resonance in air. Were this technique used in a vacuum, it would be possible to determine the internal decay of the sample.

## 1. INTRODUCTION

In 1977, Alan G. MacDiarmid of the University of Pennsylvania, Hideki Shirakawa of the University of Tsukuba, Japan, and Alan J. Heeger of the University of California, Santa Barbara synthesized the first conductive polymer. They received the Noble Prize in 2000 for this work [1]. Conductive polymers offer a world of micromechanical possibilities. These synthetic metals, as they are called, may make possible the reduction of computer chips to the micro or nanometer scale, construction of synthetic muscle, and numerous other applications by allowing conduction along a single molecule. However, such applications require an understanding of the mechanical properties of the polymer. Unfortunately, measurement of such properties is difficult because of the small size of polymer fibers and films. The goal of this research is to develop an indirect way of measuring the mechanical properties of conductive polymers.

## 2. BACKGROUND

### 2.1 Conductive Polymers

Conductive polymers are formed when a semi-conductive polymer is doped with another chemical. For instance, MacDiarmid and his associates doped polyaccetylene with halogens, increasing its conductivity by as much as 11 orders of magnitude. Similarly, doping with a variety of materials has proven to dramatically increase the conductivity of other semi-conducting fibers. Although this phenomenon is not entirely understood, it is theorized that the doping agent acts as an acceptor between monomers, allowing electrons to pass down along the polymer [1100]. Conductive polymers, like all polymers, can take a variety of different forms, of which the most relevant to this

research are films and fibers. Films can be formed with relative ease by depositing the polymer in solution onto a slide and allowing the solvent to evaporate. Fibers can be formed by spinning or electrospinning. To spin fibers the polymer is either converted to a viscous state or dissolved in a solvent. This liquid is then forced through small holes and the polymer allowed to harden. (This may be accomplished simply by allowing the fibers to cool or by allowing the solvent to evaporate but may require additional chemicals depending on the polymer.) In most cases, fibers formed in this way are next stretched to improve their molecular alignment and thus their strength [2]. This process has the disadvantage that the size of the fibers is limited by the size of the hole through which they are forced and the amount of stretching that they can undergo. As a result, such fibers are macroscopic.

Electrospinning, however, can produce fibers of the micro and nano-scale dimension. To facilitate electrospinning the polymer is dissolved in a solvent with a low boiling point, such as chloroform or water. The solution is then placed in a syringe, which is tilted at such an angle that a drop of the solution is poised at the tip of the syringe. A metal target is placed some distance from the syringe, and a voltage difference is produced between the end of the syringe and the target. This voltage produces an electric field on the surface of the drop of solution, countering the surface tension that holds the drop together. When the voltage reaches a critical level, the electric force becomes greater than the surface tension. The drop breaks down, and a jet of the solvent is emitted. The jet is accelerated toward the target by the potential difference. As it travels through the air the solvent evaporates and the single jet breaks into many smaller jets.

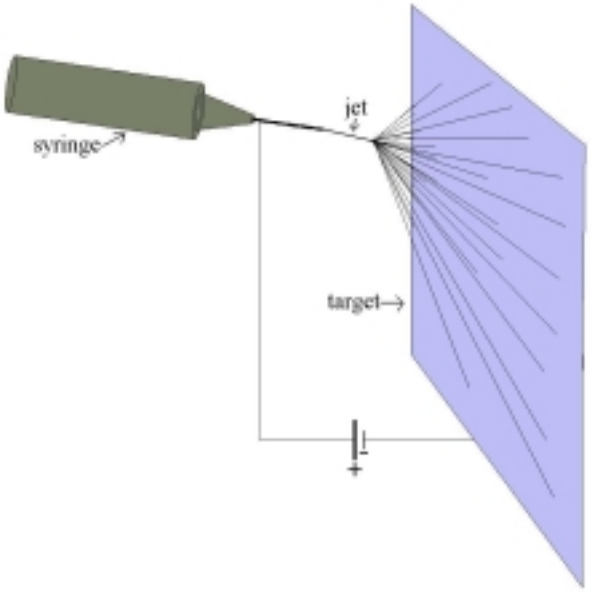


Figure 1: The electro spinning setup.

The fibers form an unwoven mat on the target and are collected. Fibers produced in this manner can have diameters on the nanometer scale [3]. However, the effectiveness of this technique is dependent on the viscosity of the solvent, which can complicate the spinning of conductive fibers.

## 2.2 Anelastic Relaxation and Internal Friction

Internal friction causes anelastic relaxation by dissipating the energy from a system. Thus, by measuring the anelastic relaxation one may calculate the internal friction. An anelastic material is one that deviates from Hook's law, which relates stress $\sigma$ and strain $\varepsilon$ ($\sigma = M\varepsilon$ or $\varepsilon = J\sigma$ with $M = 1/J$). Thus, Hook's law implies that for every stress there is a unique equilibrium strain, that this equilibrium is reached instantaneously, and that the stress-strain relationship is linear. The definition of anelasticity deviates from Hook's law in that it postulates that the equilibrium is reached only after the passage of time. Hence, when a stress is applied (or removed) from an anelastic material, it takes time for the material to reach equilibrium, or relax, and this process can be recorded [4].

One way of analyzing anelastic behavior is to periodically impose a stress and determine the strain's phase lag behind the stress. For such experiments it is convenient to use complex notation. Stress is written as $\sigma = \sigma_0 e^{i\omega t}$ where $\sigma_0$ is the stress amplitude and $\omega$ is the angular frequency ($\omega = 2\pi f$, where $f$ is the frequency). The linearity of the stress-strain relationship ensures that the strain is also periodic at the same frequency. Therefore, the strain can be written as $\varepsilon = \varepsilon_0 e^{i(\omega t - \phi)}$ where $\varepsilon_0$ is the strain amplitude, and $\phi$ is the angle by which the strain lags the stress, or the loss angle. The elastic compliance of the material in question (J) is $\varepsilon/\sigma$, a complex number, dependent only on the angular frequency since, by linearity, $\varepsilon_0/\sigma_0$ is a constant. Thus, $J(\omega) \equiv \varepsilon/\sigma = |J|(\omega)e^{-i\phi(\omega)}$, where $|J|(\omega) = \varepsilon_0/\sigma_0$.

The periodic strain can be written alternatively as $\varepsilon = (\varepsilon_1 - \varepsilon_2)\, e^{i\omega t}$ where $\varepsilon_1$ is the amplitude of the component of the strain in phase with the stress and $\varepsilon_2$ is the amplitude of the component of the strain that is 90° out of phase with the stress. Dividing by $\sigma$ gives $J(\omega) = J_1(\omega) - iJ_2(\omega)$, where $J_1(\omega)$ $(\varepsilon_1/\sigma)$is the storage compliance (or the real part of $J(\omega)$) and $J_2(\omega)$ $(\varepsilon_2/\sigma)$ is the loss compliance (or imaginary part of $J(\omega)$). From the vector diagram in Figure 2 it is easy to see that $\tan\phi = J_2 / J_1$.

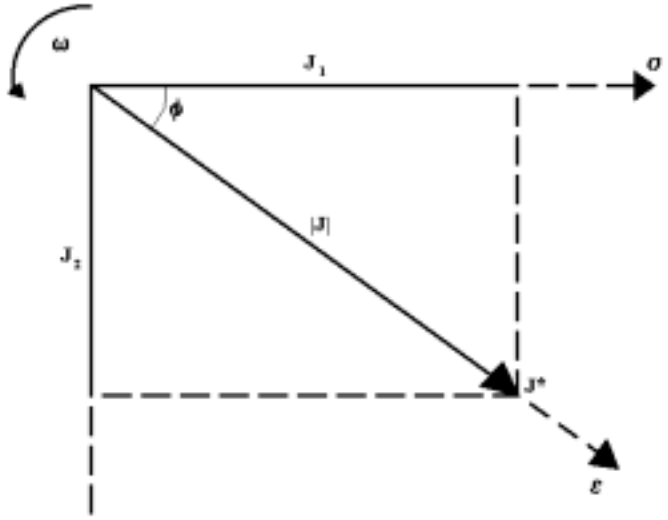


Figure 2: Vector diagram in the complex plan showing the relationship between stress, strain, and compliance.

Calculating the energy stored and the energy dissipated in a cycle of vibration demonstrates the significance of the storage and loss compliance ($J_1$ and $J_2$). The energy per unit volume at any phase of the cycle is $\int \sigma\, d\varepsilon$ between the start of the cycle and the point in question. Thus the energy dissipated through a whole cycle is $\Delta W = \int \sigma\, d\varepsilon = \pi J_2 \sigma_0^2$. The maximum stored energy occurs at $\pi/2$, $W = \int \sigma\, d\varepsilon = 1/2\ J_1 \sigma_0^2$. The ratio of the energy stored to the energy dissipated is related to the loss angle, $\Delta W/W = 2\pi\ J_2 / J_1 = 2\pi \tan\phi$. Since $\phi$ gives a measure of the fractional energy lost per cycle, it is a measure of the internal friction [10-14].

One way of determining the internal friction of a system is to measure its decay after excitation. One example of this would be a mass ($m$) on a spring. A normal decay after the driving force is removed appears in Figure 3.

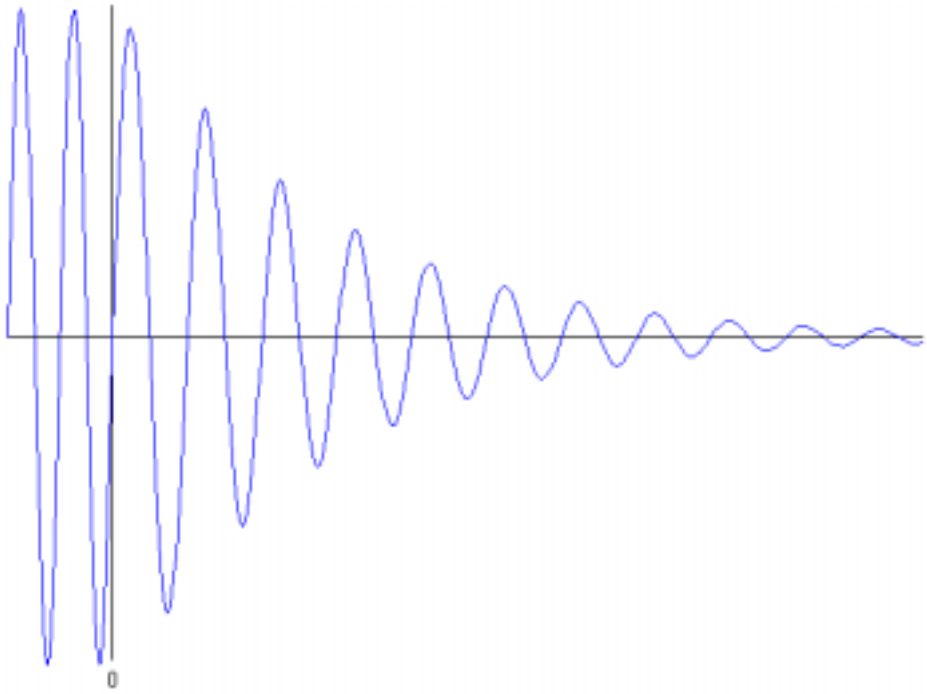


Figure 3: The decay curve when the force is removed at 0 has an exponential envelope. $A(t) = A_0 e^{-f0t\delta}$

The equation for the motion of the mass when the periodic force is applied is $mx'' = F_a - F_s$, where $m$ is the mass of the body on the spring, x is the displacement, $F_a$ is the force applied ($F_a = F_0 e^{i\omega t}$), and $F_s$ is the force within the system [$F_s = k_1(1+i\tan\phi)x$, where $k_1(1+i\tan\phi)$ is the complex spring constant]. The equation of motion for the system when the periodic force is removed (when $F_a = 0$) is $mx'' + k_1(1+i\tan\phi)x = 0$. Solving this equation yields $x = x_0 e^{i\omega t}$ and $\omega = \omega_0[1+(i\delta/2\pi)]$ or $x = x_0 e^{-\delta f t} e^{i\omega 0t} \equiv A(t)\, e^{i\omega 0t}$, where $\omega$ is the resonance frequency, $\omega_0$ is the frequency in free decay, $\delta$ is a constant, and A(t) is the envelope function, which is exponential if $\delta$ is small. Substituting into the equation of motion after the force is removed gives $\omega_0^2 = k_1/m[1-(\delta^2/4\pi^2)] \approx k_1/m$ while $\delta \approx \pi\phi$. Furthermore, $\delta$ represents the natural logarithm of the ratio of two consecutive amplitudes ($A_n$), $\delta = \ln(A_n / A_{n+1})$. Calculations are further simplified so that, except for

terms of order $\phi^2$, $\omega_0 = \omega$. To summarize the equations that are useful in determining the internal friction: $\phi = \delta/\pi = \Delta W/(2\pi W)$ when $\phi << 1$ [10–14].

## 3. EXPERIMENTAL RESULTS

The goal of this research was to measure the anelastic decay of a conductive polymer fiber from a state of resonance oscillation. The sample is forced into harmonic resonance by having a current passed through it in the presence of an oscillating magnetic field, which creates a Lorentz force that causes it to oscillate. Once the sample is at resonance, the current can be turned off and the decay envelope recorded. Then the internal friction is calculated as described above.

### 3.1 Gold Wire

Before attempting the experiment with the conductive polymer in a vacuum, I tried it using 50-micrometer gold wire in air. Vladimir Dominko, the laboratory manager of the Micro Fabrication Laboratory at the University of Pennsylvania, prepared the gold used to make the wire. It was 99.9999% pure and had a resistivity of $2.44 \times 10^{-6}$ ohms m. I mounted a length of the gold wire between two alligator clips, one fixed in a large vice and the other to the movable stage of a microscope. This allowed me to precisely adjust the tension I could place on the wire, although it did not give any sort of tension measurement. I used a coil (length: 2cm, outer diameter: 1.9cm, inner diameter: .4cm) provided by Mr. Dominko, having a inductance of 5 μH and a phase angle of 89 degrees, to create the magnetic field. I placed the coil beneath the gold wire, leaving about 1mm of clearance. I connected a Hewlett Packard 3310B function generator to the coil and a Hewlett Packard 721A DC power supply to the gold wire.

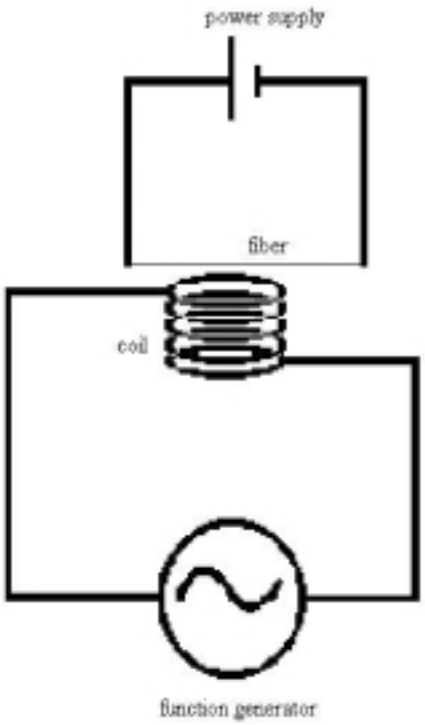


Figure 4: Experimental set-up. The signal generator and coil produce an oscillating magnetic field that causes the DC current carrying fiber to oscillate.

Using this setup I was able to oscillate the gold wire. The power supply limited the current to about 27ma, and the function generator produced about 20amps. By observing the wire through a microscope, I was able to adjust the frequency of oscillation and obtain resonance.

The purpose of this model was to establish that it was possible to place a conducting fiber into resonance oscillation. Having accomplished this, I looked at the relationship between the resonance frequency and the tension on the wire. I set the tension and found the resonance frequency by looking through the microscope and adjusting the frequency. I then changed the tension and found the new resonance frequency. I measured the tension as the change in position of the end of the gold wire, not as a force.

Theoretically the resonance frequency is proportional to the square root of the tension, because $\omega_r = \pi r/L\sqrt{(\tau/\rho)}$, where $\omega_r$ is the resonance frequency, r is the number of the harmonic, L is the length of the wire, $\tau$ is the tension, and $\rho$ is the linear density and r, and $\rho$ are constants.

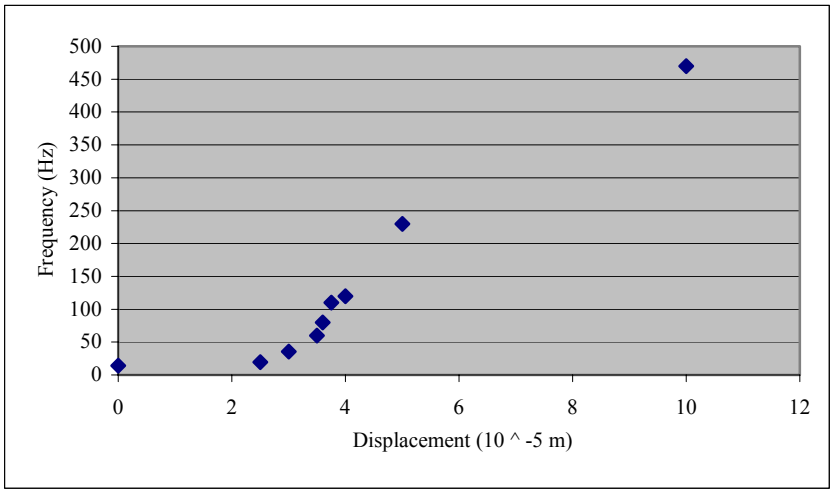


Figure 5: Frequency vs. Displacement

This is the first set of data I took. I took the data going from low tension to high tension. Thus it is possible that the inconsistency is due to the wire stretching or slipping.

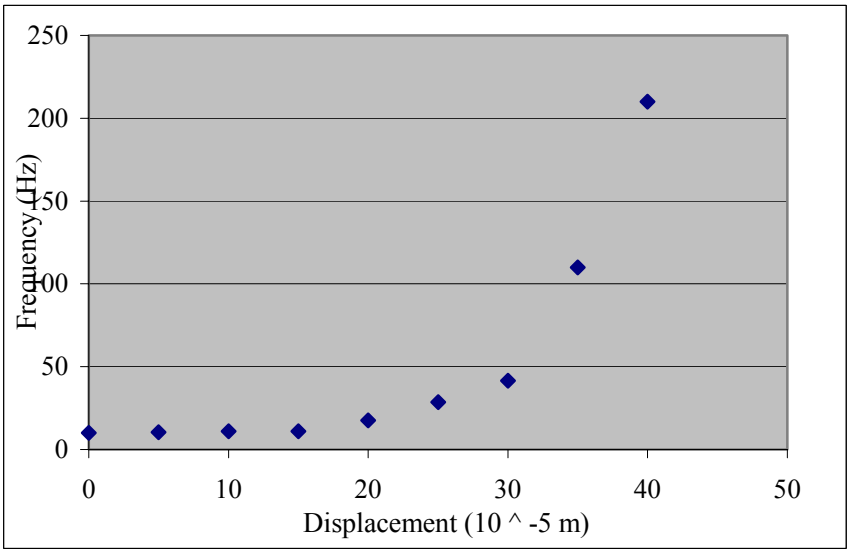


Figure 6: Frequency vs. Displacement

This is the second set of data. This time I measured from high to low tension to try to prevent slipping or stretching from affecting the results. (However, the displacement is graphed such that the lower tension coincides with lower displacement.) The data are not consistent with the theory unless it is the case that at low tension, the displacement is probably not proportional to the tension. If this is so, the data might be consistent with the lower portion of the theoretical curve.

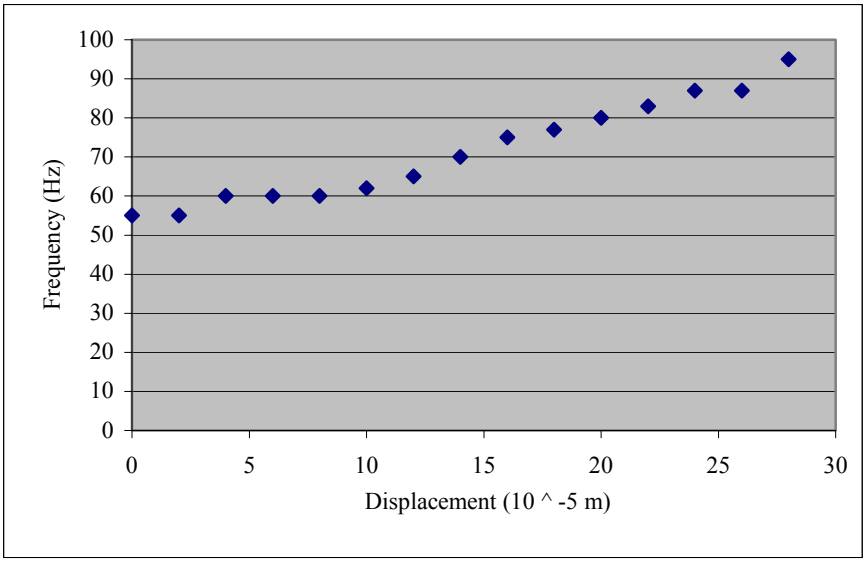


Figure 7: Frequency vs. Displacement

This last set of data appears to be more consistent with the theory; however there is still considerable deviation. This may be caused by slipping and stretching within the system, by the dampening of the air, or by the displacement not being directly related to the tension. This research established that it would be necessary to directly measure the tension of the fibers being tested.

I hoped to be able to observe the decay of the gold wire from resonance with an oscilloscope. When the current through the wire was turned off, it would continue to oscillate because of conservation of energy. This motion would then cause a voltage to be induced in the gold wire according to Faraday's law of induction, $\varepsilon = - d\Phi_B/dt$, where $\Phi_B = \iint_s \mathbf{B} \bullet d\mathbf{A}$ ($\varepsilon$ is the induced voltage, $\Phi_B$ is the flux of the magnetic field **B** through a surface of area **A**. Unfortunately, I was not able to observe any decay on the Philips PM 3052 60mHz oscilloscope. I thought that this might be due to the oscillating magnetic field. Therefore, I changed the setup so that the coil was driven by the DC power supply (thus producing a constant magnetic field) while the signal generator produced an alternating current in the gold wire. Although this proved to be an equally effective way of driving the wire, there was still no observable decay. I discussed alternatives, including optically measuring the decay, but decided to postpone following up on any of these alternatives until I had the experiment working with the conductive fibers.

### 3.2 Polymer Fibers and Films

After working with the gold wire model, I tried to get some conductive polymer fibers. Dr. Nicholas J. Pinto, who was working in the Chemistry Department at the University of Pennsylvania, prepared emeraldine (polyaniline doped with protonic acids) fibers for me. The emeraldine was dissolved in chloroform and doped with polyethylene oxide to increase its viscosity before being electrospun into fibers. When spun, the fiber formed bundles of varying diameters in a fine web, which extended from the tip of the syringe to the aluminum target. The fibers were then collected on a portable stage or a piece of

aluminum. Initially, I had some difficulty transporting and working with the fibers because they were electrostatically attracted to paper and plastic and would stick to these surfaces. To prevent this I built a movable stage from a clamp. This stage could be taken to the lab where the fibers were spun and thus the fibers could be collected directly on the stage.

Once I had the fibers, I attempted to pass current through them using the HP DC power supply. However, the fibers refused to pass any measurable current. I tried to pass a current through the fibers using a power supply capable of supplying up to 100 volts (the Electronic Measurements Co. Transitory Power Supply Model 212 A) but to no avail. After continued attempts to pass current through the fibers and other tests by Dr. Pinto, it was determined that the conductivity of the fibers was too low for any measurable current to pass.

Since the fibers were not working, Dr. Pinto recommended that I try cutting an emeraldine film into strips. Dr. Pinto made the film by placing some emeraldine-chloroform solution on a plastic slide and heating the slide on a hotplate for 24 hours to evaporate the chloroform. After being carefully removed from the slide, the film was then allowed to soak in hydrochloric acid for 24 hours. Then after drying the film flat, I cut it into strips.

The film strips were able to conduct a current of about 6 ma. If more current than this was pushed through the film, it quickly burned out and would no longer conduct. I measured the relationship between current and voltage through the film using two Hewlett Packard 3478A multimeters.

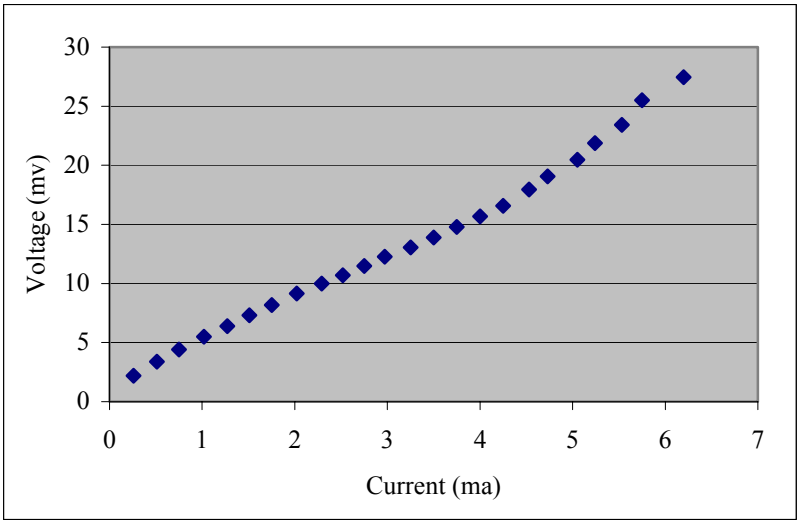


Figure 8: Voltage vs. Current 2.35cm film strip

For the first series, I used a strip of film that was 2.35cm long. The voltage-current relationship appears to be relatively linear, as would be expected from Ohm's law (V=IR). The slop of the best-fit line or resistance of this piece of film is about 4. This

gives 1.7 ohms per meter length. The y-intercept is greater than 0 (about 1) because of contact resistance.

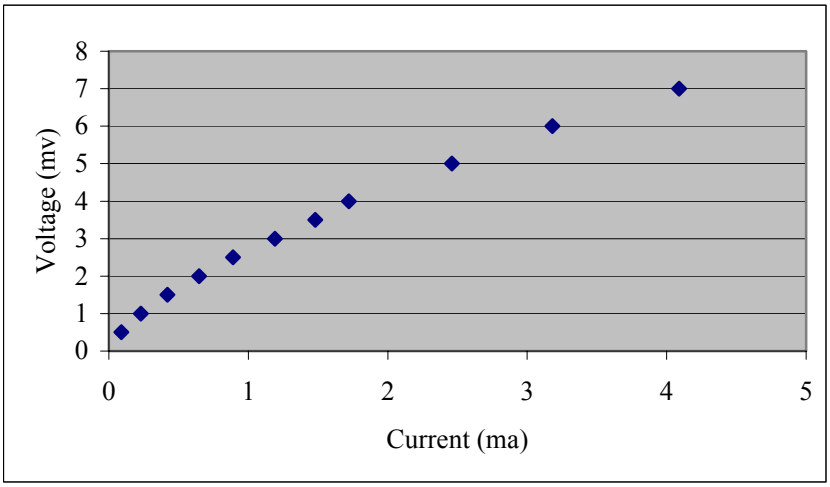


Figure 9: Voltage vs. Current 1.4 cm film

I repeated the experiment using a 1.4cm piece of film. The resistance of this piece was about 1.6 ohms, giving a resistance of 1.1 ohms per meter, considerably less than in the first experiment. This discrepancy is probably due to inconsistency in the thickness of the film and in the width of the strips. The contact resistance was .88 ohms, which is slightly less than in the first trial.

Next, I tried to get the film to oscillate. Unfortunately, because the film was stiff, it would not oscillate. I got a bigger coil (length: 2.5cm, outer diameter: 10cm, inner diameter: 4.4cm), thus increasing the magnetic field and the force on the film. The bigger coil also had the advantage that the film could be placed inside it, where the field was stronger and more uniform. Nonetheless, I could not get the film to oscillate. I cut a wider strip of film, hoping that it would conduct more current, but it actually conducted less. This was probably because the strip of film was thinner than the previous pieces.

### 3.3 OPTICAL MEASUREMENT OF ANELASTIC DECAY

Because of time limitations, I decided to leave the conductive polymer and focus on developing the technique for measuring the decay from resonance and thus the internal friction. While developing this technique, I used graphite fibers, which I collected from a broken fishing pole. These fibers were far more conductive than the emeraldine film, conducting between 8 and 50 milliamps depending on their diameter. Furthermore, they were far more compliant than the film and were easily forced into oscillation.

To measure the decay, I used a red light emitting diode (LED) and a photosensitive transistor. The voltage across the emitter and collector of a phototransistor is inversely related to the light incident on the base. Thus, when the fiber oscillates between the light source (the LED) and the transistor, the voltage increases because the fiber blocks the

light. As the fiber's oscillations decay from resonance, the fiber blocks less light and the voltage decreases.

The gain or change in voltage of the transistor is affected by the initial voltage across the transistor and the resistance in the circuit. The gain can be dramatically increased by increasing the resistance on the emitter side of the transistor. I set up the following circuit as shown in Figure 10.

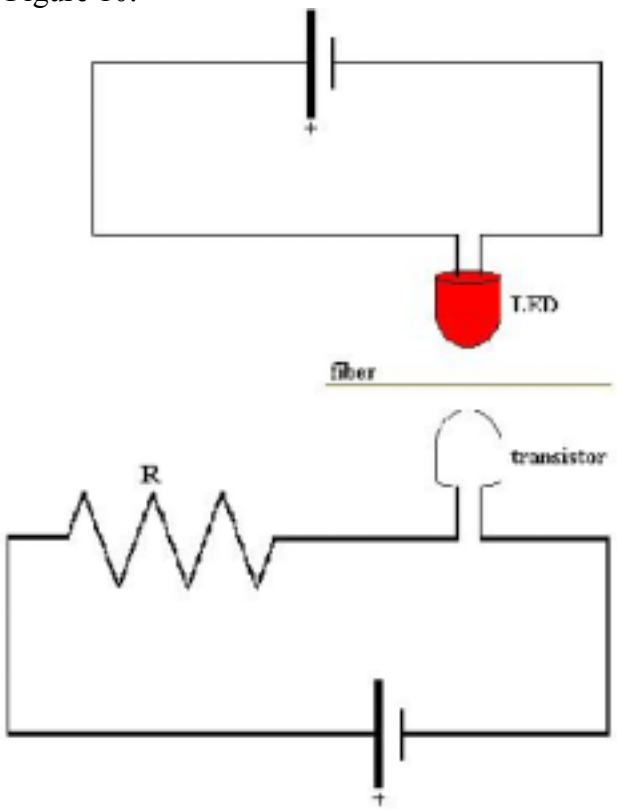


Figure 10: Setup for optical measurement of decay from resonance
In this figure, the fiber would be oscillating into and out of the page.

Both the transistor and LED were driven by DC power supplies. The voltage across the LED was adjusted so that the light was bright but the LED did not burn out. The voltage across the transistor was set to about 5 volts. Using lens wax, I fixed the LED and transistor into a movable mount so that there was about a centimeter between them for the fiber (see Figure 10). I aligned them so that the voltage deflection was at a maximum. I then positioned the LED and transistor, in their mount, on the fiber stage so that the fiber was just at the edge of the LED.

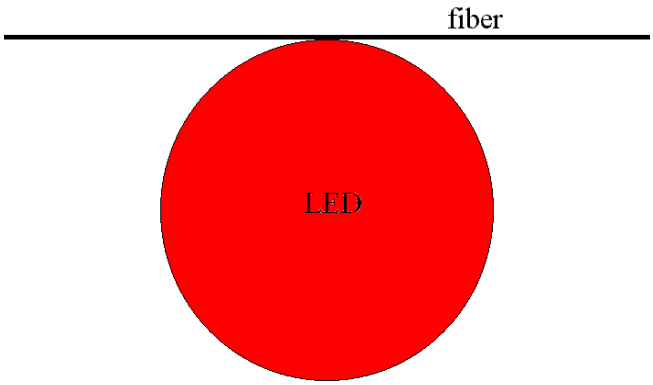


Figure 11: Fiber LED alignment.
In this figure, the fiber would be oscillating up and down.
Thus, as it decays from resonance it will block less and less light.

I then placed the entire setup inside the large coil, passing direct current through the fiber and alternating current through the coil. When the current through the fiber was turned off, there was a noticeable jump in the voltage. Unfortunately this jump was not large enough to measure. This situation was worsened by a considerable amount of noise. I tried to increase the size of the fluctuation by increasing the resistance on the emitter side of the transistor from about 18Ω to about 28Ω. Additionally, I tried to eliminate the noise by switching from an oscillating magnetic field to an oscillating current through the fiber, but this did not prove to be effective.

In the hope of increasing the voltage gain caused by the oscillating conductor, I switched from the graphite fibers to the 50μm diameter gold wire. Using wire between 3 and 4 cm in length I was able to increased the amplitude of the harmonic wave and thus get a significant voltage gain. By setting they oscilloscope to the 50m and .5 sec scale, I was able to observe the decay of the voltage. Unfortunately, there was a significant amount of noise.

I hoped to eliminate the noise from the system by using a double T filter.

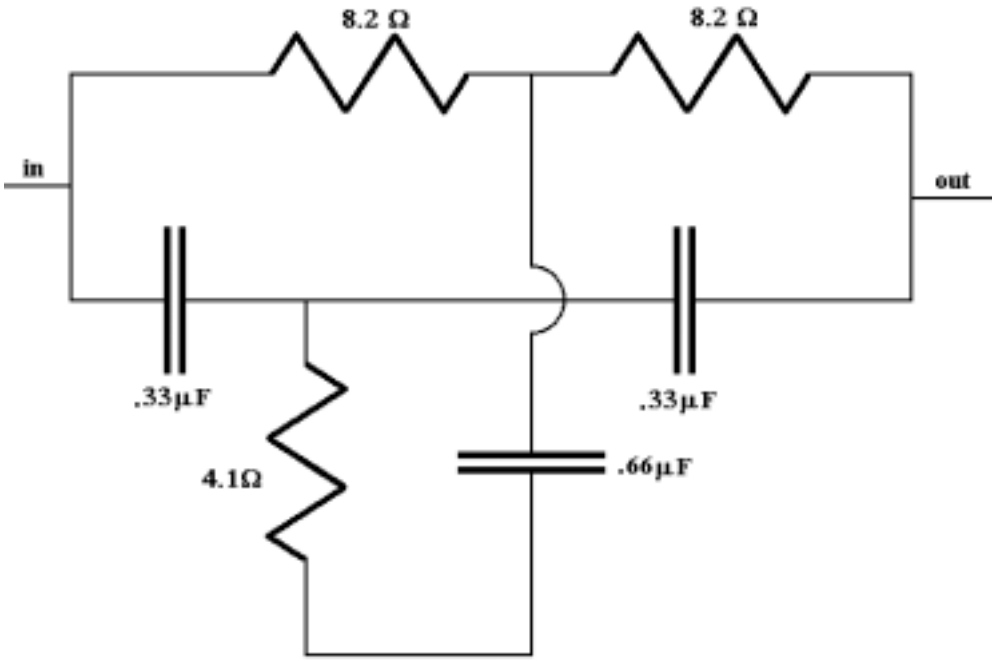


Figure 12: Double T filter

Although this eliminated the noise, it also reduced the voltage gain so that the decay was not visible. However, I believed that the decay envelope could be recorded despite the noise. Unfortunately, due to time limitations, I was not able to attempt this.

## 4. DISCUSSION AND CONCLUSIONS

Although this research was hampered by difficulties with materials and time constraints, the value of further research in this area is clear. The measurement of the decay to determine the internal friction would be conducted in a vacuum to eliminate dampening effects. Optical measurement of the decay might be improved by the use an infrared LED, which might improve the voltage gain to a point where the decay becomes visible. Alternatively, a lens could be used to focus the light from the LED onto the transistor. Another option would be to use a laser rather than an LED, which would have the advantage of giving a more highly condensed beam. However, such refinements do not appear to be necessary currently.

## 5. ACKNOWLEDGMENTS

I would like to thank Dr. Jorge Santiago-Avilés for his guidance and support, without which this research would not have been possible. Additional thanks go to Dr. Nicholas J. Pinto for providing the conducting polymer for this research. Furthermore, I would like to thank Vladimir Dominko, Sid Deliwala, and George Hunka for materials and advice. Finally, I would like to extend my deepest gratitude to the National Science Foundation for their support of undergraduate research through the SUNFEST-REU program.

## 6. REFERENCES


1. C.K. Chiang, C.R. Fincher, Jr., Y.W. Park, A.J. Heeger, H. Shirakawa, E.J. Louis, S.C. Gau, and A.G. MacDiarmid, Electrical conductivity in doped polyacetylene, *Phys. Rev. L*, 39 (1977) 1098-1101.
2. A.Y. Grosberg and A.R. Khokhlov, *Giant Molecules: Here, There, and Everywhere*, Academic Press, New York, 1997, p. 28-32.
3. J.N. Doshi, *The Electrospinning Process and Applications of Electrospun Fibers,* UMI Dissertation Services, Ann Arbor, 1997, p. 7-20.
4. A S. Norwick and B.S. Berry, *Anelastic Relaxation in Crystalline Solids*, Academic Press, New York, 1972, p1-3.


## 7. BIBLIOGRAPHY


A P. Arya, *Introduction to Classical Mechanics*, Prentice Hall, Upper Saddle River, 2nd ed., 1998.

A.N. Cleland and M.L. Roukes, Nanoscale mechanics, http://ww.cmp.caltech.edu/~roukes/papers/cleland4.pdf. G. Genta, *Vibration of Structures and Machines: Practical Aspects*, Springer-Verlag, New York, 2nd ed., 1995.

K.F. Graff, *Wave Motion in Elastic Solids*, Dover Publication, New York, 1975.

R. Harberman, *Elementary Applied Partial Differential Equations with Fourier Series and Boundary Value Problems*, Prentice Hall, Upper Saddle River, 3rd ed., 1998.

J.B. Merion and S.T. Thornton, *Classical Dynamics of Particles and Systems*, Saunders College Publishing, Philadelphia, 4th ed., 1995.

E.M. Purcell, *Electricity and Magnetism, Berkeley Physics Course*, Vol. 2, McGraw-Hill Book Company, New York, 1965.

R.A. Serway, *Physics for Scientists and Engineers,* Saunders College Publishing, Philadelphia, 1996.

E.W. Wong, P.E. Sheehan, and C.M. Lieber, Nanobeam mechanics: elasticity, strength and toughness of nanorods and nanotubes, *Science*, 277 (1997) 1971-1975.